A hybrid APSO–ANFIS optimization based load shifting technique for demand side management in smart grids

Mohamed Faradji[1], Toufik Madani Layadi[2], Khaled Rouabah[3]

[1]LIST Laboratory, Department of Electrical Systems Engineering, University of M'Hamed Bougara, Boumerdes, Algeria
[2]Laboratory of Materials and Electronic Systems, Department of Electromechanical, Faculty of Sciences and Technology, University Mohamed El Bachir El Ibrahimi of Bordj Bou Arreridj, El Anceur, Algeria
[3]Department of Electronics, University of M'sila, University Pole, M'sila, Algeria

Article Info

ABSTRACT

Cost and performance are considered important parameters to obtain an optimized configuration for smart grids. In this paper, a new optimization approach, based on a hybrid adaptive particle swarm with an adaptive neuro-fuzzy inference system (ANFIS) algorithm, has been proposed. This approach allows optimizing demand side management (DSM) using the load shifting technique. The impact of the latter on consumer profile, electricity pricing mechanisms, and overall grid performance are illustrated. In this simulation, the focus lies on modeling DSM using a day-ahead load shifting approach as a minimization problem. Simulation experiments have been tested separately on three different demand zones, namely, residential, commercial, and industrial zones. A comparative study of solutions was performed, focusing on both reduced peak demand and operational costs. The obtained results demonstrate that the optimization presented in this article approach outperforms the other approaches by achieving greater savings in the residential and commercial sectors. The study proved a significant reduction in peak demand. In fact, values of 23.76%, 17.61% and 16.5% in peak demand reduction are achieved in the case of residential, commercial, and industrial sectors, respectively. Furthermore, operational cost reductions of 7.52%, 9.6%, and 16.5% are obtained for the three different cases.

Corresponding Author:

Mohamed Faradji
LIST Laboratory, Department of Electrical Systems Engineering, University of M'Hamed Bougara
35000, Avenue de l'Indépendance, Boumerdes, Algeria
Email: m.faradji@univ-boumerdes.dz

1. INTRODUCTION

Increasing penetration of renewable energy sources and the growing complexity of modern power grids have led to the emergence of smart grids, enabling more efficient and sustainable energy management [1]. In smart grids, the demand side management (DSM) strategy plays a crucial role in balancing the electricity supply. This strategy allows autonomous management for consumers. Also, the DSM strategy aims to optimize energy consumption patterns and peak loads and enhance grid reliability. The DSM strategy is based on many different techniques. The most effective DSM technique, which involves the adjustment of electricity consumption timing without altering the overall energy consumption level, is called "load shifting". DSM optimization via load shifting improves energy efficiency, reduces costs, and enhances grid stability by transferring consumption from peak to off-peak hours, benefiting utilities and consumers with lower bills and promoting sustainability [2].

Many techniques have been developed recently, leading to cost savings and peak load reduction for appliances in different parts of smart grids. Layadi *et al.* [3] proposed optimization strategy considers fuel costs and aims to reduce greenhouse gas emissions. The hybrid regenerative power system (HRPS), powered by a central energy management system (CEMS), efficiently supports critical AC/DC loads and is improved by regenerative technology [4]. The study [5], [6], a summary of some techniques, based on linear and dynamic programming, has been discussed in much detail. However, these techniques are considered less efficient when the number of loads is important. Different methods like the mixed integer linear programming referenced in [7], and the non-linear mixed-integer wind driven optimization (WDO) mentioned in [8], have been applied to manage flexible and time-shiftable home devices. A study in [9] compares the harmony search algorithm (HSA) with the firefly algorithm (FA), finding that the FA is superior for reducing the peak-to-average ratio (PAR) while the HSA excels in cost-effectiveness. The usefulness of this study could be enhanced by including data on how quickly each algorithm converges. This paper [10] introduces a DSM framework that utilizes the ant colony optimization (ACO) approach within a smart grid context. Nonetheless, the ACO method initially faced issues with early convergence. The convergence process was refined by incorporating a mutation mechanism into the standard ACO algorithm [11]. Consequently, this modified approach is employed to achieve cost reductions and lower the PAR.

The implementation of DSM using a genetic algorithm (GA) has been used to allocate residential loads. The objective here is to enhance user satisfaction and minimize energy costs simultaneously. This approach involves deriving a cost-per-unit satisfaction index, which serves as an estimator for user satisfaction during load shifting [12]. Load shifting DSM was applied to traditional, smart, and solar photovoltaic (PV)-integrated homes using binary particle swarm optimization (BPSO), GA, and Cuckoo search algorithms, resulting in reduced peak loads and costs, with the Cuckoo search algorithm outperforming the others [13].

The study presented in [14] uses the GA for DSM to lower peak loads in an industrial DC micro-grid with solar power and batteries. Significant peak load and cost reductions were achieved, benefiting various sectors. A DSM strategy using the moth flame optimization (MFO) algorithm effectively reduced peak loads in residential and commercial areas [15]. Binary grey wolf optimization (BGWO) algorithm outperforms BPSO in optimizing residential electrical appliances, significantly reducing energy costs and lowering peak loads and PAR [16]. A hybrid GA-PSO algorithm is harnessed to effectively curtail energy costs through the optimal allocation of generations and loads in a day-ahead market [17]. Notably, PSO exhibits superior performance over GA in this context.

In the scope of DSM techniques, diverse strategies including load shifting, peak clipping, valley filling, strategic conservation, and strategic load growth have been employed to modify consumer load behavior [18]. The core objective is to reduce peak energy demand by shifting it to off-peak times. Utilities can directly control consumer loads or indirectly guide consumers to self-manage usage, with incentives for compliance and penalties for non-compliance. Pricing schedules encourage consumption adjustment. Several techniques for demand-side management in smart grids are available as depicted in Figure 1 including, load shifting: moving energy use from peak to off-peak times; peak clipping: cutting down peak energy demand; valley filling: using extra energy during low-demand periods; load building: reshaping energy use to increase efficiency; strategic conservation: encouraging energy-saving behaviors; and flexible load management: working with consumers to adjust their energy use, offering incentives for cooperation. These methods enhance grid resilience and efficiency. However, load shifting stands out as the most extensively explored technique in existing literature [19]. The study's simulation shows that DSM, as a minimization problem using the adaptive moth flame optimization (AMFO) algorithm, effectively reduces peak loads and energy costs in various sectors [20].

These studies focus on cost reduction in smart grids and home energy systems across various sectors, using optimization algorithms like BGWO and HSA, as well as the utilization of symbiotic organisms search (SOS) and Cuckoo search (CS) algorithms [21]. Optimized energy storage and management are critical for effective DSM in smart grids [22]. They enable load balancing by storing excess energy during low-demand periods and releasing it during peak times, which reduces grid stress and operational costs. This optimization enhances demand response programs, promotes renewable energy integration, and allows consumers to participate in energy arbitrage, leading to cost savings and greater grid resilience [23]. By reducing reliance on the grid during high-demand periods, optimized storage strengthens DSM's role in ensuring a stable and efficient energy system [24]. A multi-objective optimization model for hybrid power systems, considering fuel cost variations and employing various algorithms, has been created [25]. Additionally, a tool to estimate the lifespan of lead-acid batteries in these systems is developed. A comparative study between lithium and lead-acid batteries in hybrid multi-source systems is developed [26].
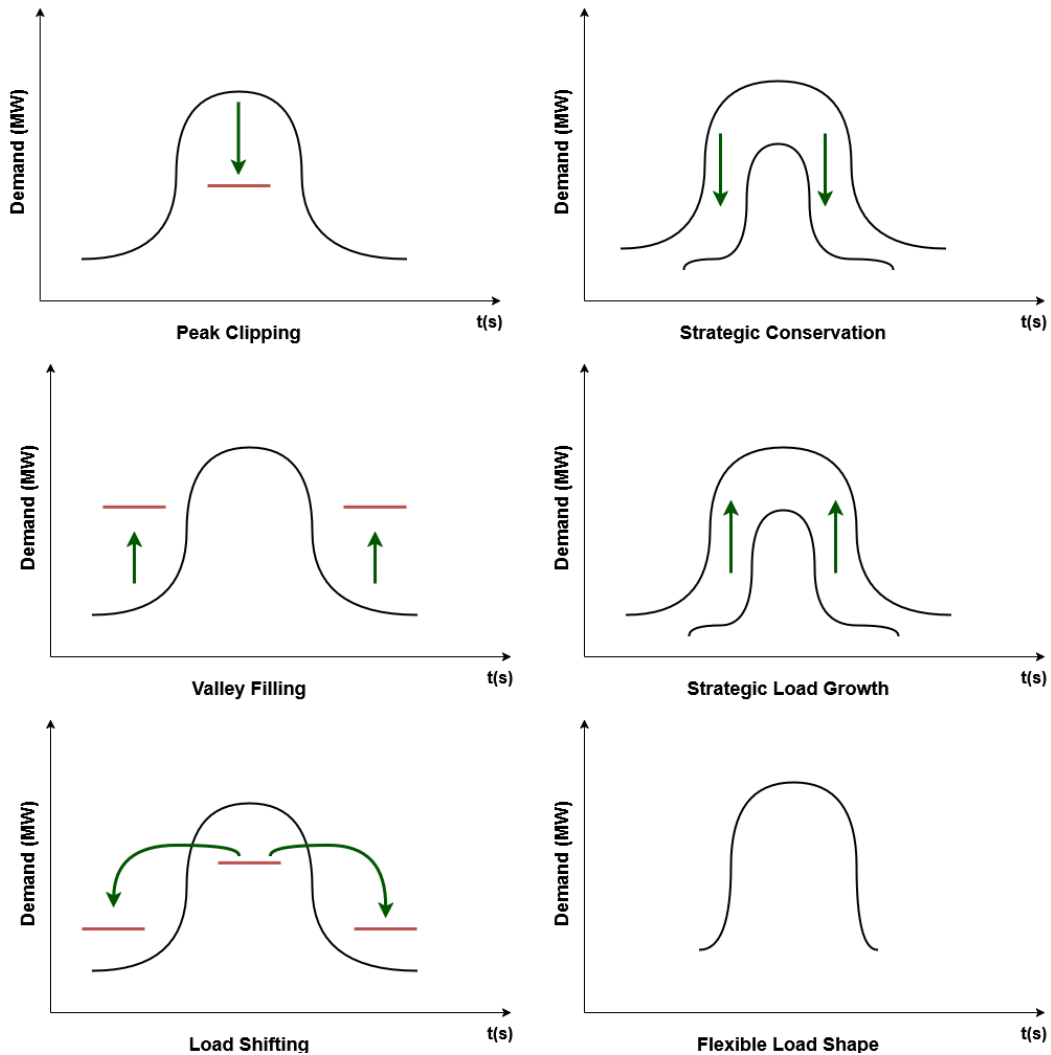
Figure 1. DSM techniques

The present paper focuses on optimizing DSM using the load shifting technique in smart grids. It explores the impact of load shifting on consumer behavior, electricity pricing mechanisms, and overall grid performance. Among the examined papers, certain authors have focused on optimizing the cost-minimization objective function, while others concentrated solely on minimizing peak loads. These objective functions can be categorized as single-objective minimization problems. In the context of a single objective, optimizing costs inherently leads to a reduction in peak loads, and vice versa optimizing peak loads contributes to decreased energy costs. Some researchers have investigated the amalgamation of renewable energy with DSM within home energy management systems.

However, when dealing with vast areas and a multitude of devices, the integration of renewable energy with DSM has not been extensively explored thus far. Through a comprehensive review of existing literature, case studies, and simulation-based analyses, this article aims to provide an effective adaptive PSO strategy. An algorithm-based load shifting technique is used to reduce operational costs and peak demand in different consumption areas. The findings and recommendations presented in this paper demonstrate the advancement of DSM strategies, enabling stakeholders to make informed decisions regarding load shifting optimization and ultimately fostering a more sustainable, reliable, and economically efficient smart grid ecosystem. The need for integrating adaptive neuro-fuzzy inference system (ANFIS) in adaptive PSO is that this method can outperform PSO alone by combining the strengths of both methods. PSO, a global optimization algorithm, is effective at exploring complex, multi-dimensional search spaces and finding optimal solutions, but it can sometimes struggle with slow convergence or getting trapped in local optima, particularly in highly non-linear systems. On the other hand, ANFIS integrates neural networks with fuzzy inference systems, allowing it to model complex, non-linear relationships by learning from data and adjusting

itself accordingly. In the PSO–ANFIS hybrid, PSO optimizes the parameters of the ANFIS model, such as fuzzy membership functions, while ANFIS refines these results through adaptive learning based on real-world data. This hybrid approach provides the advantages of global search from PSO and local tuning from ANFIS, resulting in faster convergence, improved accuracy, and better adaptability to changing or uncertain environments. Figure 2 illustrates the use of an intelligent algorithm for DSM in a smart grid. This algorithm optimizes the balance between electricity supply and fluctuating consumer demand, a critical aspect of modern grids due to the increasing reliance on variable renewable energy. By analyzing real-time data, the smart algorithm adjusts DSM strategies to manage these fluctuating loads, ensuring grid stability and efficiency. The smart grid network, equipped with advanced communication and automation technologies, enables real-time interaction between energy providers and consumers, allowing for dynamic adjustments that reduce peak demand, improve energy utilization, and enhance overall grid performance. The organization of this paper is given as follows: the methods summarizing the main keys of the contribution are presented in section 1. Also, the problem formulation is illustrated. Section two is concerned with the description of simulation scenarios, modeling, and simulation data organization. The proposed algorithm of optimization and optimization diagram are given in section three. The results of the simulation are discussed in section four. Finally, a conclusion is presented summarizing the findings, and discussing the implications.
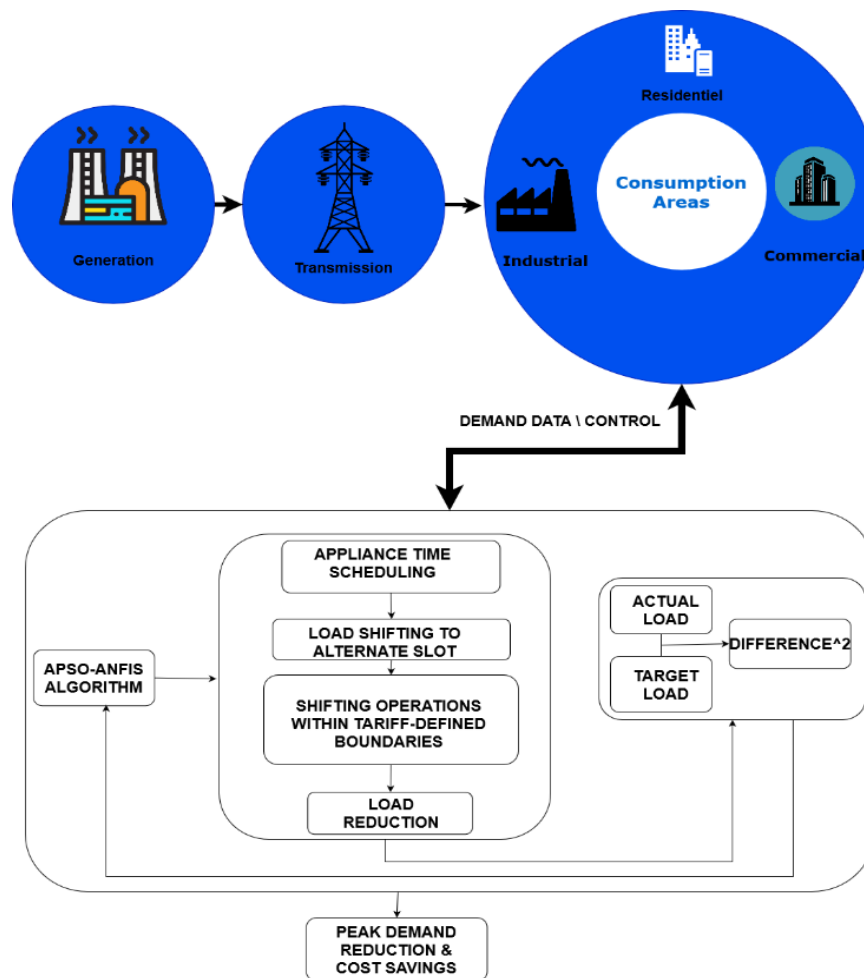

Figure 2. Application of a smart algorithm for DSM within a smart grid network that handles fluctuating loads

2. MATERIALS AND METHODS

The suggested method introduced in this paper consists of investigating optimization of the DSM in various smart grid areas, including residential, commercial, and industrial sectors. The smart grid is integrated with the primary grid, operating at a voltage of 410 V. The link lengths for the different sectors are

2 km for residential, 3 km for commercial, and 5 km for industrial zones. Uniform market prices for electricity are applied to all sectors within the smart grid. By analyzing and optimizing energy consumption in these distinct sectors, this study aims to contribute valuable insights into effective load management and cost-saving strategies within smart grid environments.

Figure 2 depicts the (DSM) framework within a multi-sector smart grid. In this framework, energy is provided to three sectors: residential, commercial, and industrial, all sourced from the grid. The optimization introduced in this study is a multi-strategy adaptive PSO load shifting technique for the aforementioned DSM. The modelling and simulation of the smart grid as well as the optimization algorithm implemented in this study are implemented on MATLAB software. Figure 2 shows a general description of the proposed approach.

The proposed strategy for demand management revolves around implementing load shifting measures on appliances. The objective is to optimize the load consumption profile, bringing it as closely aligned as possible with the predetermined objective load curve. To achieve this alignment, a specific minimization equation is employed as part of the strategy:

$$\sum_{t-1}^{T} (S_{load}(\text{t}) - \text{objective}(t))^2 \qquad (1)$$

In this context, $S_{load}(\text{t})$ signifies the real energy usage at the time (t), and '$objective(t)$' indicates the targeted energy usage at that same moment. The cumulative energy usage at the time (t) is determined by summing up the predicted load for that time with the loads that were either connected or disconnected before the load shifting operation. The load's mathematical expression is presented as (2).

$$S_{load}(t) = S_{forcasted}(t) + S_{connected}(t) + S_{disconnected}(t) \qquad (2)$$

The term "Connection(t)" means the load increment at a time "t" resulting from the adjustment of connection time to that specific moment. It encompasses both the load increase at a time "t" caused by devices scheduled for times preceding "t" and the load increases due to the shifting of their connection. The connection formulation is shown in (3).

$$\text{Connection (t)} = \sum_{m=1}^{t-1} \sum_{n=1}^{M} G_{nmt}.C_{1n} + \sum_{v=1}^{k-1} \sum_{m=1}^{t-1} \sum_{n=1}^{M} G_{nm(t-1)}.B_{(1+v)n} \qquad (3)$$

Where, G_{nmt} represents the count of devices of type "n" that are shifted from instance "m" to "t". The variable "M" denotes the device type. C_{1n} and $B_{(1+v)n}$ correspond to the power consumption of device type "n" at time instances 1 and $(1 + v)$, respectively. The variable "k" signifies the total duration of consumption for devices of type "n". The term "Disconnection(t)" refers to the reduction in load caused by delayed connection timings of devices, which were originally scheduled to start their consumption at a time "t". It also encompasses the load decrease resulting from delayed connection times of devices that were expected to commence consumption at times preceding "t". The mathematical expression of the disconnection term is given as (4).

$$\text{Disconnection (t)} = \sum_{x=t+1}^{t+y} \sum_{n=1}^{M} G_{ntx}.B_{1n} + \sum_{v=1}^{k-1} \sum_{X=t+1}^{t+y} \sum_{n=1}^{M} G_{n(t-1)x}.B_{(1+v)n} \qquad (4)$$

In the provided equations, G_{ntx} denotes the number of devices of type "n" that have been transferred from time instance "t" to "x". To clarify the process of load shifting, Figure 3 displays the timeframes during which loads are connected or disconnected. There are two categories of loads: fixed and movable. Fixed loads remain constant and unalterable within their original periods, while movable loads can be rescheduled to different time slots due to their controllable characteristics.

In Figure 3, the loads are initially depicted according to their original operating schedules before any connection or disconnection events. The shift in loads is illustrated after the disconnection phase has been completed. This problem is structured as a minimization challenge, with the stipulation that the device count should never be allowed to become negative. To satisfy this condition, the number of available controllable devices G_{nmt} should consistently exceed the count of devices meant to be shifted away G_{nmt} at any given moment, which is expressed by (5).

$$\sum_{t=1}^{T} G_{nmt} < Bt\ (n) \qquad (5)$$

$Bt_{(n)}$ denotes the count of devices of type "n" available for control at time instance "j".
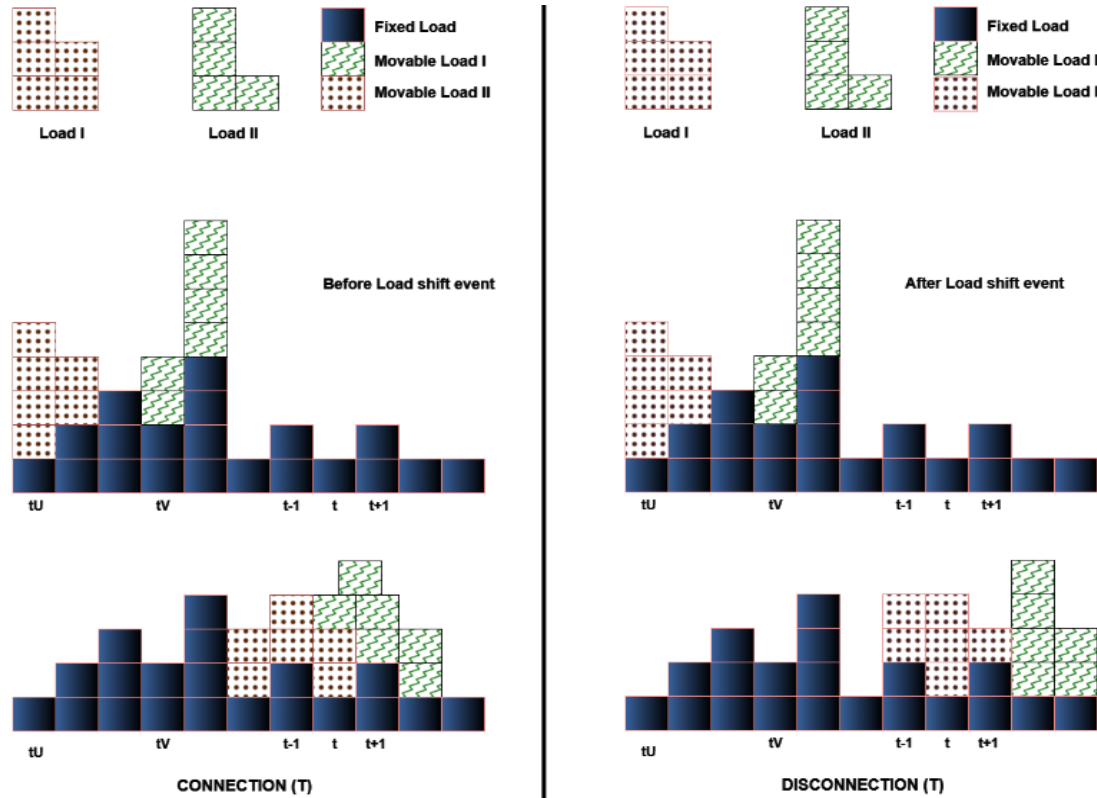
Figure 3. Connection and disconnection of loads in DSM

3. DESCRIPTION OF SCENARIOS FOR SIMULATION

The study was carried out across various sectors of the smart grid, including residential, commercial, and industrial zones. Operating alongside the main grid, the system functions at a voltage level of 410 V. The sectors are positioned at distances of 2 km, 3 km, and 5 km, respectively. A uniform market price is applied across all sectors. The primary aim is to reduce utility costs by structuring the objective function to be inversely related to the market price.

The power demand for the residential, commercial, and industrial sectors is 1.5 MW, 2 MW, and 3 MW, respectively. It is important to note that electricity demand is lower during off-peak morning hours, typically before 8 am. As a result, this period is excluded from high-peak load shifting. The time window for load shifting begins at the eighth hour of the current day and continues into the next day.

The objective function, which seeks to maximize consumer savings, is modeled as the inverse of electricity prices [19]. This is represented by (6) in the study, with the goal of reducing electricity costs for utility companies by setting the objective curve opposite to the market price.

$$Objective\ function = \frac{S_{avg}}{S_{max}} \times \sum_{t=1}^{24} ForcastedLoad \times \frac{1}{S(t)} \tag{6}$$

In this context, S_{avg} refers to the average electricity price over a 24-hour period, S_{max} denotes the maximum price during this time, and $S(t)$ represents the price at any given time "t". This study takes into account the energy consumption of various types of devices, considering factors such as the number of device types within the system, the daily operational hours for each device type, the maximum duration a device can operate continuously, the forecasted load for each type, the initial-hour consumption, continuous operation hours, and the start time for each device.

Table 1 outlines the hourly electricity consumption predictions for residential, commercial, and industrial microgrids, alongside the corresponding wholesale electricity prices (in cents per kWh) throughout the 24-hour period where the first hour is 8.00 - 9.00 AM. Each hour is matched with a specific wholesale price and the projected energy consumption (in kWh) for each microgrid category. This table is useful for analyzing load patterns and price dynamics across different sectors in the grid.

Table 1. Forecasted load consumption data categorized by zones

Time	Wholesale price (ct/kWh)	Forecasted hourly load (kWh)		
		Residential microgrid	Commercial microgrid	Industrial microgrid
1st hour	12	729.4	923.5	2045.5
2nd hour	9.19	713.5	1154.4	2435.1
3rd hour	12.27	713.5	1443	2629.9
4th hour	20.69	808.7	1558.4	2727.3
5th hour	26.82	824.5	1673.9	2435.1
6th hour	27.35	761.1	1673.9	2678.6
7th hour	13.81	745.2	1673.9	2678.6
8th hour	17.31	681.8	1587.3	2629.9
9th hour	16.42	666	1558.4	2532.5
10th hour	9.83	951.4	1673.9	2094.2
11th hour	8.63	1220.9	1818.2	1704.5
12th hour	8.87	1331.9	1500.7	1509.7
13th hour	8.35	1363.6	1298.7	1363.6
14th hour	16.44	1252.6	1096.7	1314.9
15th hour	16.19	1046.5	923.5	1120.1
16th hour	8.87	761.1	577.2	1022.7
17th hour	8.65	475.7	404	974
18th hour	8.11	412.3	375.2	876.6
19th hour	8.25	364.7	375.2	827.9
20th hour	8.1	348.8	404	730.5
21th hour	8.14	269.6	432.9	730.5
22th hour	8.13	269.9	432.9	779.2
23th hour	8.34	412.3	432.9	1120.1
24th hour	9.35	539.1	663.8	1509.7

3.1. Residential case

The operational scope of this region encompasses household appliances characterized by modest power consumption and limited operating durations. A total of 2,600 controllable devices, spanning across 14 distinct types, compose this inventory. Table 2 provides a comprehensive overview of these controllable devices, alongside their corresponding consumption data.

Table 2. Controllable device data in the residential area

Type	Device's hourly consumption (kW)			
	1st	2nd	3rd	Device
Dryer	1.2	-	-	189
Dish washer	0.7	-	-	288
Washing machine	0.5	-	-	268
Oven	1.3	-	-	279
Iron	1	-	-	340
Vacuum cleaner	0.4	-	-	158
Kettle	2	-	-	406
Toaster	0.9	-	-	48
Rice cooker	0.85	-	-	59
Hair dryer	1.5	-	-	58
Blender	0.3	-	-	66
Frying pan	1.1	-	-	101
Coffee maker	0.8	-	-	56
Total	-	-	-	2605

3.2. Commercial case

In contrast, the commercial domain showcases higher utilization ratings in comparison to the residential sector. Here, over 800 devices representing 8 diverse types contribute to the potential for load management. Table 3 provides a detailed overview of these controllable devices and their associated energy usage figures.

3.3. Industrial case

Within this context, the industrial sector maintains a notably smaller device count when juxtaposed with the broader spectrum of controllable devices; however, it compensates with substantial consumption levels and extended device operational durations. Industrial devices within this zone exhibit prolonged continuous operation, often critical regardless of load control methodologies. Within this scope, a collection of 100 controllable devices spanning 6 distinct types emerges. These devices, alongside their respective consumption data, are enumerated in Table 4.

Table 3. Controllable device data in the commercial area

Type	Device's hourly consumption (kW)			
	1st	2nd	3rd	Device
Water dispenser	2.5	-	-	156
Dryer	3.5	-	-	117
Washing machine	0.5	-	-	268
Kettle	3	2.5	-	123
Oven	5	-	-	77
Coffee maker	2	2	-	99
Air conditioner	4	3.5	3	56
Lights	2.5	1.75	1.5	87
Total	-	-	-	808

Table 4. Controllable device data in the industrial area

Type	Device's hourly consumption (kW)						
	1st	2nd	3rd	4th	5th	6th	Device
Water heater	12.5	12.5	12.5	-	-	-	39
Welding machine	25	25	25	25	-	-	35
Fan AC	30	30	30	30	-	-	16
Arc furnace	50	50	50	50	50	50	8
Induction motor	100	100	100	100	100	100	5
DC motor	150	150	150	-	-	-	6
Total	-	-	-	-	-	-	109

4. A HYBRID APSO–ANFIS OPTIMIZATION ALGORITHM

The presented PSO-fuzzy hybrid algorithm integrates PSO and fuzzy logic to tackle optimization problems. Initiated by setting parameters for both PSO and fuzzy logic, the algorithm initializes particles with random positions and velocities. In the main PSO loop, fitness is evaluated, and personal and global best positions are updated based on the objective function. Notably, the algorithm incorporates fuzzy logic by using each particle's position as input to a fuzzy logic system, influencing the particle's position update. This integration enhances adaptability and accommodates uncertainties within the optimization process. The global best position and value, representing the optimized solution, are displayed at the conclusion of the iterations. The algorithm's strength lies in the collaborative decision-making synergy between PSO's global optimization and fuzzy logic's interpretability, making it effective for navigating complex search spaces and addressing problems with inherent uncertainties.

4.1. A multi-strategy adaptive particle swarm optimization algorithm

An effective DSM technique should be capable of handling a variety of controllable loads, each with unique characteristics. Linear programming and dynamic programming prove inadequate for managing a considerable number of diverse loads simultaneously [27]. The PSO algorithm functions as a population-based stochastic search technique. Within this framework, each particle's position signifies a potential solution to the optimization problem at hand. Evaluation of a particle's position occurs through an assessment of its merit, quantified by the fitness value extracted from the optimization function. In the initialization phase of the PSO algorithm, the particle population is randomly established as a collection of candidate solutions. Subsequently, each particle traverses the search space at a specific velocity, subject to dynamic adjustments based on its individual flight history and that of its companions [27].

The algorithm converges toward the optimal solution through iterative cycles until the predefined convergence condition is satisfied. This iterative refinement process collectively contributes to the attainment of the most favorable solution. PSO stands as an intelligent algorithm exhibiting global convergence, minimizing the need for extensive parameter adjustments. Nonetheless, conventional PSO encounters challenges like susceptibility to local optima and gradual convergence. The hybrid APSO–ANFIS optimization algorithm (HAPA) addresses these issues by mitigating the search process's inherent limitations, leading to enhanced convergence precision and speed. This adaptation empowers the algorithm to efficiently tackle intricate optimization problems, reducing search process bias and enhancing its suitability for complex scenarios [27]. The velocity expression of the algorithm is given in (7), and the estimated position is illustrated by (8).

$$v_i(t + 1) = \omega \times v_i(t) + c1 \times rand() \times \left(p_i(t) - x_i(t)\right) + c2 \times rand() \times \left(g_{best}(t) - x_i(t)\right) \quad (7)$$

$$x_i(t + 1) = x_i(t) + v_i(t + 1) \quad (8)$$

Where "x" is the supposed population with "n" particles is the velocity of ith particle, $p_i(t)$ signifies the personal best position that particle "i" has encountered since the initial time step. Furthermore, "g_{best}" designates the most optimal position discovered by the collective particles up to that point in the process. In this context, where i ranges from 1 to D, certain variables are defined. The inertia weight is represented as "ω", with "c1", and "$c2$" serving as constants intrinsic to the PSO algorithm and taking values within the range of [0,2]. Meanwhile, "$rand$()" stands for random numbers confined within the interval [0,1]. An illustrative representation of the particle movement process based on PSO iterations is presented in Figure 4.
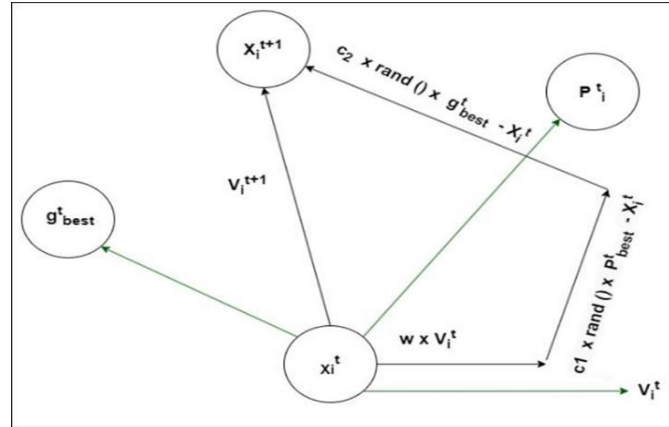

Figure 4. A sequential progression of particle motion within the PSO framework

The strategies for enhancing inertia weights "ω" and learning factors ($c1, c2$) encompass a spectrum of classifications, including constancy or stochasticity, linearity or non-linearity, and adaptability. Existing research has experimentally demonstrated the efficacy of non-linearly decreasing weights over linearly decreasing ones within the context of the dual dynamic adaptation mechanism. The utilization of nonlinear learning factors offers heightened compatibility with intricate optimization objectives, aligning well with the complexities inherent in such pursuits. A noteworthy approach leverages inertia weights to fine-tune learning factors, thereby achieving a balance between individual particle learning capabilities and collective group learning capabilities. This equilibrium significantly enhances the algorithm's optimization accuracy. In this paper, a hybrid approach amalgamating both strategies has been adopted, yielding superior results. The flowchart depicted in Figure 5 demonstrates the proposed optimization algorithm. The parameter "ω" serves as a pivotal determinant influencing the performance and efficacy of the PSO algorithm. Reduced values of "ω" bolster the algorithm's capacity for local search, elevating convergence accuracy. Conversely, larger "ω" values enhance global search capabilities, preventing particles from being confined to local optima; however, this might result in a slower convergence rate. A significant proportion of ongoing enhancements in PSO pertain to the optimization of "ω".

$$\omega = \omega_{min} + (\omega_{min} + \omega_{min}) \times \exp[-20 \times (\tfrac{t}{T})^6] \tag{9}$$

Where T is the maximum number of time steps, usually. The learning factor ($c1, c2$) varies according to "ω". The values of "$c1$" and "$c2$" within the velocity update equation plays a crucial role in determining the degree of learning exhibited by a particle toward its optimal position. Specifically, "$c1$" governs the degree of self-learning of the particle, while "$c2$" influences the extent of its social learning. These coefficients also contribute to altering the particle's trajectory over time.

Building upon prior insights, this study adopts an enhanced adjustment strategy for these learning factors and inertia weights. This strategy capitalizes on the advantages of employing non-linear functions. The coefficients are harmonized with the values "A = 0.5", "B = 1", and "C = 0.5", resulting in formula 10. By leveraging this refined combination, the PSO algorithm can achieve improved performance and convergence outcomes. Formulations of the factors "C1" and "C2" are respectively given by (10) and (11).

$$C1 = A\omega2 + B\omega + C \tag{10}$$

$$C2 = 2.5 + C1 \tag{11}$$

The algorithm's convergence and the speed at which it converges are significantly intertwined with the position weighting factor. However, the primary parameter-tuning approach often concentrates solely on refining velocity updates, neglecting position updates. To address this limitation and regulate the impact of velocity on position, an innovative position update formula incorporates a constraint factor "α". The introduction of "α" serves the purpose of calibrating the influence of velocity, aiming to mitigate search process limitations and subsequently enhance the algorithm's convergence rate.

In the basic PSO framework, a particle's new position is determined by adding its current velocity to its present position. However, the direct addition of position and velocity vectors requires the introduction of a constraint factor within the position update formula. Traditionally, this constraint factor in the PSO algorithm is typically set to 1. The role of "α" is to steer the particle toward proximity to its optimal position, and its enhancement controls the degree to which velocity influences position. By regulating this influence, the algorithm's convergence is notably enhanced. In this study, an "α" that evolves based on changes in ω is employed. During the initial stages, "α" is heavily influenced by particle velocity, facilitating robust exploration. Subsequently, in later stages, α's sensitivity to particle velocity diminishes, reinforcing its efficacy in local search activities.

$$x_{ij}(t + 1) = x_{ij(t)} + \alpha\, v_{ij(t+1)} \tag{12}$$
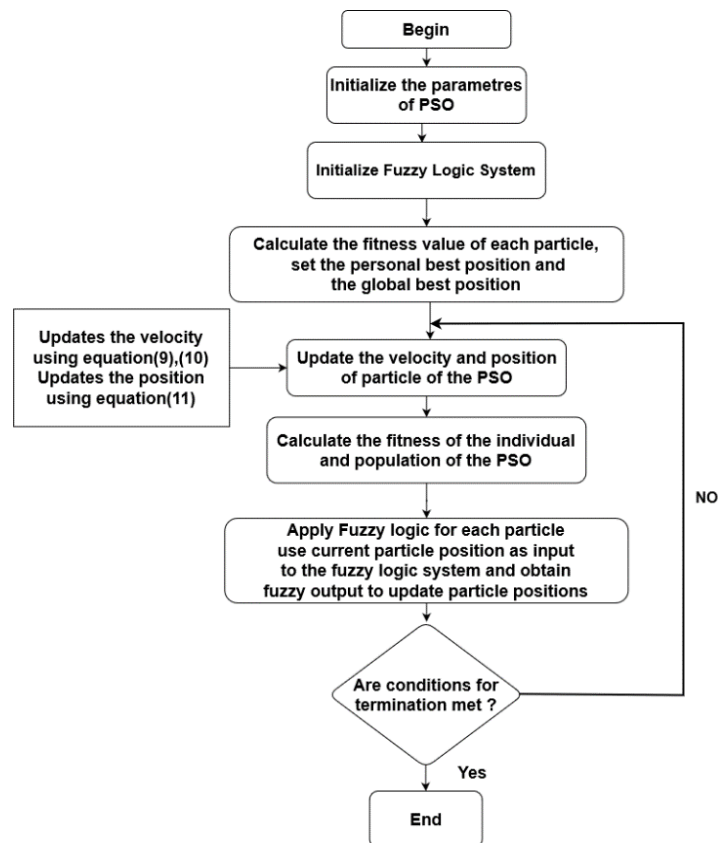
$$\alpha = 0.1 + \omega \tag{13}$$

Figure 5. Flowchart for HAPA algorithm

4.2. An adaptive network-based fuzzy inference system

Neural networks (NN) represent potent and versatile tools for forecasting, leveraging simplicity alongside remarkable capabilities. Their effectiveness hinges on the availability of sufficient training data, a judicious selection of input-output samples, an appropriate number of hidden units, and ample computational resources. Notably, NN possesses the ability to approximate any nonlinear function and tackle

problems with ill-defined or challenging-to-compute input-output relationships, owing to their data-driven nature [28].

Predictive models benefit from multi-layer feedforward neural networks that utilize sigmoid activation in the hidden layers and linear activation for the output layers. Concurrently, fuzzy logic systems provide a nonlinear conversion of input arrays into single output values, integrating both quantitative data and verbal insights. A standard fuzzy logic system includes four main parts: a fuzzifier, a set of rules, an inference engine, and a defuzzifier. The fuzzifier converts precise input values into fuzzy terms, using membership functions to express how closely a variable relates to a certain characteristic. Fuzzy rules, formulated as 'if-then' propositions, can be based on empirical data or the linguistic expertise of specialists.

The Mamdani and Sugeno inference systems serve as essential tools and vary in their methodologies. The Mamdani system transforms fuzzy input values into fuzzy output values, whereas the Takagi-Sugeno model associates fuzzy inputs with definite outputs. Subsequently, the defuzzifier translates fuzzy values into precise numbers based on different measures such as the area's centroid, area's bisector, average of maximum values, or the utmost value. The Figure 6 depicts the structure of an ANFIS controller. It shows the integration of fuzzy logic and neural networks to create a hybrid control system. This structure allows the ANFIS controller to adapt and improve its performance over time, making it effective for complex, nonlinear control tasks.
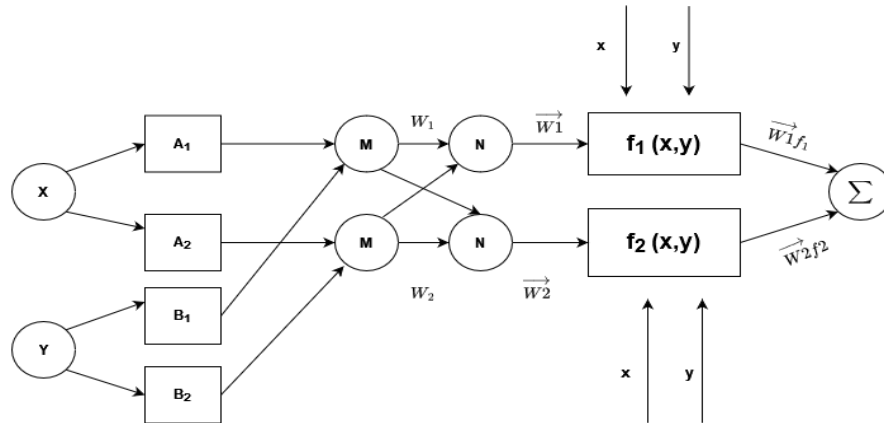

Figure 6. Block diagram of ANFIS controller

Despite the automatic knowledge acquisition during the learning process, NN functions as a "black box," making it challenging to extract knowledge from them. In contrast, fuzzy systems are more interpretable through their rules, though defining these rules becomes intricate with numerous variables and complex relations. Combining NN and fuzzy systems provides a synergistic advantage. In a neuro-fuzzy system, NN automatically derives fuzzy rules from numerical data, and through the learning process, adaptively adjusts membership functions [29].

ANFIS, which belongs to the class of adaptive multi-layer feedforward networks, is used for nonlinear prediction tasks, leveraging historical data to forecast future values. It merges the autonomous learning capabilities of neural networks with the descriptive power of fuzzy inference systems. The structure of ANFIS includes five distinct layers, each consisting of nodes characterized by specific node functions, with Oji representing the output from the ith node in the jth layer.

The ANFIS architecture combines two intelligent techniques: artificial neural networks (ANN) and fuzzy logic. ANFIS is often regarded as an adaptive network closely associated with ANN. The foundation of neuro-fuzzy modeling is rooted in a unified framework known as the adaptive network, which integrates both neural network and fuzzy model concepts [29].

5.   RESULTS AND DISCUSSION

These simulations were executed using the MATLAB platform, and the load profile was sourced from [30]. The simulation outcomes vividly illustrate the effectiveness of the introduced DSM technique. Table 5 depicts the parameters used for simulation for APSO.

The technique proved the capability to substantially curtail the aggregate usage of end consumers, closely approximating the pre-defined objective load curve across all sectors within the smart grid.

Furthermore, the algorithm showcased its adeptness in efficiently managing a diverse array of loads. The depiction of the search space pertinent to the optimization function, facilitated by the HAPA algorithm, is presented in Figure 5. The objective curve depicted in black in Figure 7 to 9 is a representation of the (6).

Table 5. APSO parameters

APSO parameter	Value
Maximum iterations	50
Velocity clamping factor	2
Cognitive constant	2
Social constant	2
Number of particles	20

5.1. Residential area case

The results of applying HAPA optimization to the residential case are shown in Figure 7, Figure 7(a) illustrates the simulation outcomes for the proposed DSM technique applied within the residential domain. The graph showcases a conspicuous reduction in peak demand during the interval spanning from 10 am to 3 pm a period characterized by heightened load owing to a surge in active appliances.

This reduction is achieved by strategically redistributing the load to timeframes of diminished consumption, notably from 7 pm to 12 pm. However, it should be highlighted that the effectiveness of the algorithm is constrained during times when there is little variation in load, like the early hours before 10 am. This indicates that the optimized load for shifting is confined to an array defined by the anticipated load and the load curve applied in the optimization process.

Figure 7(b) displays the convergence pattern of the HAPA algorithm applied in the residential context. It reveals a smooth convergence trajectory, stabilizing around the 15th iteration following an initial rapid convergence phase. The Figure 7 illustrates the effectiveness of the DSM approach, which substantially reduces peak demand during the period from 10 am to 3 pm when the system experiences maximum load due to a high number of appliances in the ON state. The load is intelligently shifted to periods of lower consumption, typically from 7 pm onwards. Significantly, the application of the HAPA technique leads to a substantial 7.25% reduction in the electricity bill, decreasing from 2302.9 to 2135.94. This notable financial enhancement underscores the efficiency and cost-saving potential of the HAPA technique when implemented in residential settings.

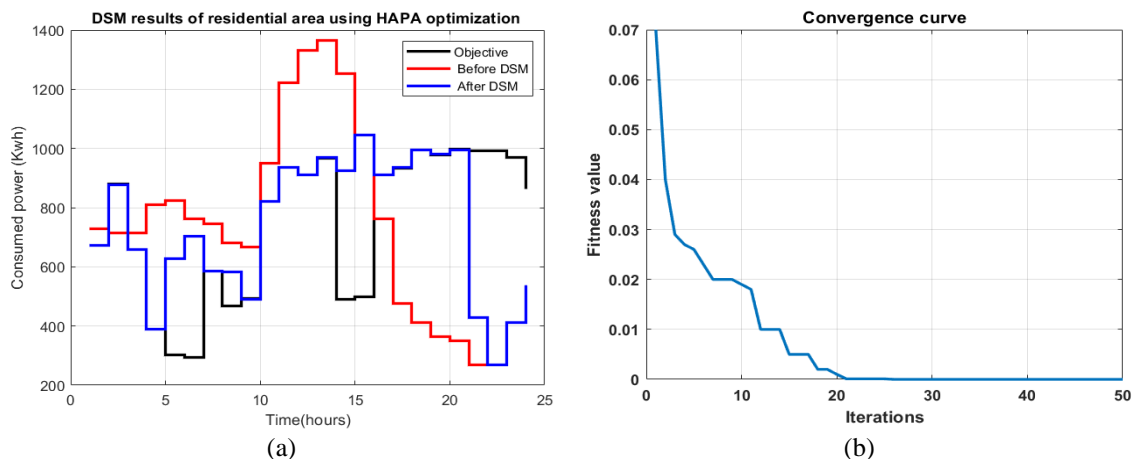(a)   (b)

Figure 7. DSM results of the residential area using HAPA optimization (a) optimized power consumption over a 24-hour period for residential area and (b) convergence curve of HAPA optimization for residential area

5.2. Commercial area case

The results of applying HAPA optimization to the commercial case are shown in Figure 8, Figure 8(a) illustrates the simulation outcomes regarding the proposed DSM technique within the commercial sector. The convergence trajectory of the HAPA algorithm for the commercial sector is depicted in Figure 8(b),

showcasing a smoother convergence pattern. After an initial swift convergence phase, the algorithm stabilizes smoothly over 11 iterations, indicating improved convergence behavior compared to the residential sector.
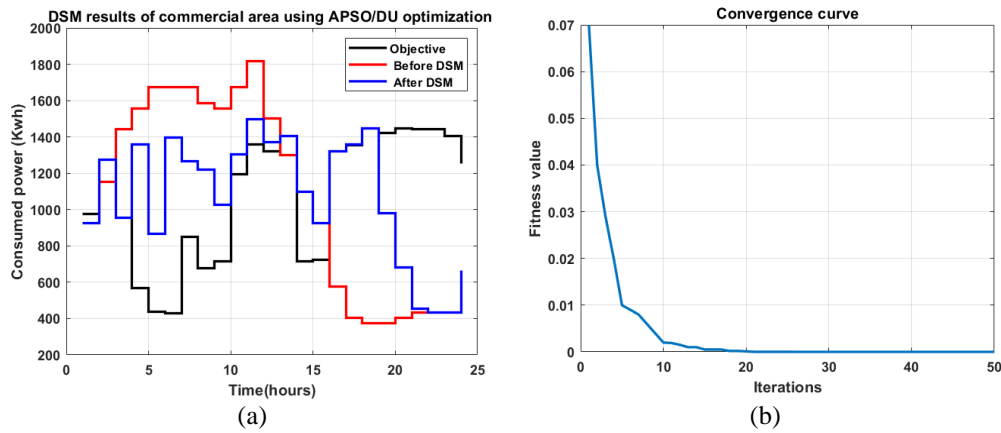

Figure 8. DSM results of the commercial area using HAPA optimization (a) optimized power consumption over a 24-hour period for commercial area and (b) convergence curve of HAPA optimization for commercial area

Notably, the application of DSM leads to a reduction in peak demand during the 10 am to 4 pm interval a time when system load is at its zenith due to numerous appliances operating. Interestingly, during low consumption windows, such as 7 pm to 12 pm, the efficacy of DSM is comparatively diminished compared to the residential sector. The algorithm's limitations are more pronounced when dealing with minimal load variations, as experienced in early morning periods before to 10 am. Remarkably, the utilization of the adaptive PSO dual-update (HAPA) technique results in a significant 9.6% reduction in the electricity bill declining from $3636.6 to $3315.12. This financial enhancement underscores the potential of HAPA in achieving cost savings within the commercial context.

5.3. Industrial area case

Shifting focus to the industrial domain, the results of applying HAPA optimization to the industrial case are shown in Figure 9, Figure 9(a) outlines the simulation outcomes for the proposed DSM technique. Given the industrial sector's substantial loads, the algorithm's efficacy is notably less competitive in curbing consumption during this time frame. The convergence trajectory of the HAPA algorithm within the industrial sector is displayed in Figure 9(b), showcasing a convergence pattern that, although not entirely smooth, ultimately reaches a minimum value after 22 iterations.
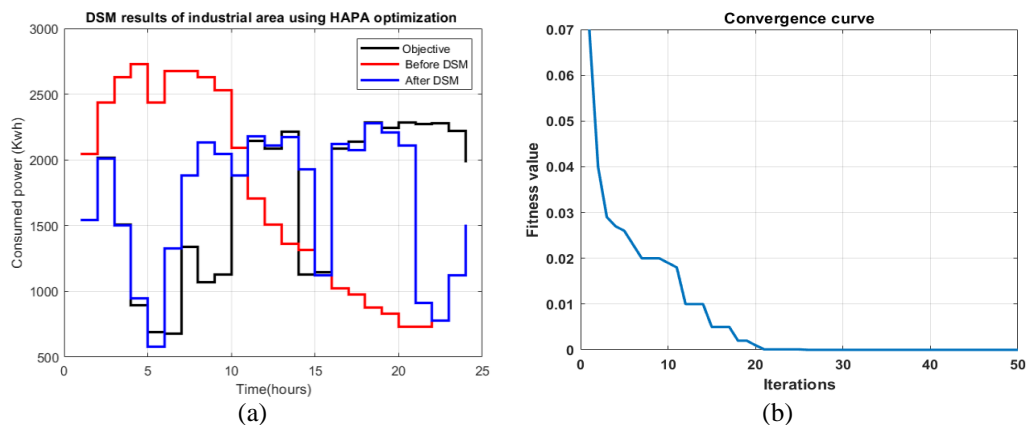

Figure 9. DSM results of the industrial area using HAPA optimization (a) optimized power consumption over a 24-hour period for industrial area and (b) convergence curve of HAPA optimization for industrial area

The summarized results of the PSO for load consumption across all three sectors are compiled in Table 6. Table 1 displays the load data prior to the implementation of DSM and the targeted load for all scenarios, accompanied by time-of-use (TOU) rates, which remain consistent across all regions. In this analysis, the maximum load recorded in the residential, commercial, and industrial sectors is 1,363.6 kWh, 1,818 kWh, and 2,727.3 kWh respectively, with the total loads amounting to 17,666.21 kWh, 25,656.55 kWh, and 40,470.70 kWh.

Table 6. HAPA optimized results for forecasted load

Time	Wholesale price (ct/kWh)	HAPA optimized forecasted load (kWh)		
		Residential microgrid	Commercial microgrid	Industrial microgrid
1st hour	12	673	977.5	1541.9
2nd hour	9.19	878.8	1276.4	2013.4
3rd hour	12.27	658.2	956	1508
4th hour	20.69	390.3	566.9	894.3
5th hour	26.82	301.1	437.3	689.9
6th hour	27.35	295.3	428.8	676.5
7th hour	13.81	584.8	849.4	1339.8
8th hour	17.31	466.5	677.6	1068.9
9th hour	16.42	491.8	714.3	1126.8
10th hour	9.83	821.5	1193.3	1882.3
11th hour	8.63	935.8	1359.2	2144
12th hour	8.87	910.4	1322.4	2086
13th hour	8.35	967.2	1404.8	2215.9
14th hour	16.44	491.2	713.5	1125.5
15th hour	16.19	498.8	724.5	1142.8
16th hour	8.87	910.4	1322.4	2086
17th hour	8.65	933.6	1356.1	2139.1
18th hour	8.11	995.8	1446.4	2281.5
19th hour	8.25	978.9	1421.8	2242.8
20th hour	8.1	997	1448.1	2284.3
21th hour	8.14	992.1	1441	2273.1
22th hour	8.13	993.3	1442.8	2275.9
23th hour	8.34	968.3	1406.5	2218.6
24th hour	9.35	863.7	1254.5	1978.9

Table 6 summarizes the HAPA's refined outcomes for energy consumption in these three sectors. It can be observed that the new peak loads are 997.0 kWh, 1448.1 kWh, and 2284.3 kWh respectively showcasing how the HAPA is successful in reducing load peaking considerably. The HAPA enhances the efficiency of energy use across all three smart grid areas, leading to cost savings. The projected energy demands for each of the three sectors, based on the same rate of electricity pricing, are detailed in the table. The HAPA algorithm efficiently optimizes load consumption and leads to expenditure reduction in all three smart grid sectors.

A comparative study with previous findings has been summarized in Tables 7 to 9 commencing with Table 7, which outlines the reduction in operational cost across different sectors, it is observed that the hybrid APSO–ANFIS optimization technique demonstrates significant effectiveness. In the residential sector, operational costs are reduced by 7.52%, while the commercial and industrial sectors experience even more substantial reductions at 9.6% and 16.83%, respectively. These findings highlight the economic advantages of implementing the proposed technique in managing and optimizing energy consumption.

Table 7. Reduction in operational cost

Sector	Cost without DSM	Cost with DSM	Reduction percentage
Residential	2,302.9	2,135.94	7.52
Commercial	3,636.6	3,315.12	9.6
Industrial	5,712	4,750.67	16.83

Moving to Table 8, which provides insights into the reduction in peak demand, the hybrid APSO–ANFIS approach continues to showcase its prowess. In the residential sector, a notable reduction of 23.25% in peak demand is achieved. Similarly, the commercial and Industrial sectors witness reductions of 17.61% and 16.5%, respectively. These results underscore the technique's adaptability across various sectors, contributing to the efficient management of peak electricity demands.

This study compared our results with those of previous findings. To ensure a fair comparison, several critical factors are accurately considered. First, a problem formulation is aligned precisely, ensuring

consistency across studies. Second, we matched simulation conditions to guarantee comparability. Lastly, we meticulously accounted for data input consistency. By adhering to these stringent criteria, it is confidently evaluated the congruence and divergence between our results and the existing literature mentioned in Table 9.

Table 9 consolidates the analysis by presenting a comprehensive comparison with previous findings. Focusing on reduction percentages of peak demand and operational costs, the HAPA method consistently outperforms other established techniques (APSO/DU, EA, AMFO) across all sectors. Noteworthy is the peak demand reduction in the residential sector at 23.76%, reinforcing the technique's efficacy in diverse household settings. Additionally, the HAPA method achieves a substantial reduction of 14.81% in operational costs within the Industrial sector, emphasizing its economic benefits.

Table 8. Reduction in peak demand

Sector	Peak load without DSM	Peak load with DSM	Reduction	Reduction percentage
Residential	1,363.6	1,046.56	317.04	23.25
Commercial	1,818.2	1,498.01	320.18	17.61
Industrial	2,727.3	2276.6	450.7	16.5

Table 9. Comparison with previous findings

Sector	Reduction percentage of peak demand				Percentage of operational cost			
	APSO/DU	EA	AMFO	HAPA	APSO/DU	EA	AMFO	HAPA
Residential	23.25	18.3	21.74	23.25	7.25	4.976	5.12	7.52
Commercial	17.61	18.3	19.74	17.61	8.84	5.83	4.9	9.6
Industrial	11.5	14.2	13	16.5	13.5	9.98	5.2	16.83

In conclusion, the hybrid APSO–ANFIS optimization technique emerges as a robust solution for DSM in smart grids. Its demonstrated effectiveness in reducing both peak demand and operational costs positions it as a valuable tool for enhancing energy efficiency and economic savings across residential, commercial, and industrial sectors. The sequential analysis of Tables 7 to 9 provides a nuanced understanding of the technique's multifaceted contributions to smart grid management. Further validation through real-world implementations could solidify its standing as a significant advancement in the field.

the HAPA optimization approach has the potential to ameliorate this scenario. The results of the simulation highlight significant savings for consumers and benefits for utility companies, including improved grid reliability and better management of electricity demand. Consumer cost savings fall within the range of 7.5–16.83%, while generation companies experience improved grid stability and optimized load management. The HAPA algorithm mitigates search process blindness, enhancing both the accuracy and speed of convergence in the algorithm. This adaptability significantly improves its performance when addressing intricate optimization problems.

6.   CONCLUSION AND PERSPECTIVES

In this paper, a new hybrid optimization algorithm has been proposed to optimize important performances in smart grids. The simulation tests were conducted across three distinct smart grid categories: domestic, business, and manufacturing sectors (residential, commercial, and industrial). These profiles are considered as loads and consumption patterns. The proposed optimization algorithm is based on hybridization between demand-side management and multi-strategy adaptive PSO techniques.

The hybrid optimization algorithm has demonstrated its effectiveness in enhancing the control parameters of the smart grid's distribution network, leading to notable improvements. In this research, a population-based metaheuristic technique was developed as a minimization method. The study demonstrates a significant reduction in peak demand by using a hybrid optimization algorithm (HAPA). Values of 23.25%, 17.61%, and 16.5% are achieved in the case of residential, commercial, and industrial sectors, respectively. Furthermore, operational cost reductions of 7.52%, 9.6%, and 16.83% are obtained for the three different cases. As a perspective work, to improve the proposed algorithm convergence a new vision has been suggested. Also, the optimization study will be extended to a large scale of smart grids.

FUNDING INFORMATION

AUTHOR CONTRIBUTIONS STATEMENT

Name of Author	C	M	So	Va	Fo	I	R	D	O	E	Vi	Su	P	Fu
Mohamed Faradji	✓	✓	✓	✓	✓	✓		✓	✓	✓			✓	
Toufik Madani Layadi		✓		✓	✓	✓		✓		✓	✓	✓	✓	
Khaled Rouabah		✓		✓		✓				✓	✓	✓	✓	

C	:	**C**onceptualization	I	:	**I**nvestigation
M	:	**M**ethodology	R	:	**R**esources
So	:	**So**ftware	D	:	**D**ata Curation
Va	:	**Va**lidation	O	:	Writing - **O**riginal Draft
Fo	:	**Fo**rmal analysis	E	:	Writing - Review & **E**diting

Vi	:	**Vi**sualization
Su	:	**Su**pervision
P	:	**P**roject administration
Fu	:	**Fu**nding acquisition

CONFLICT OF INTEREST STATEMENT

The authors declare that they have no known competing financial interests, personal or professional relationships that could have appeared to influence the work reported in this paper.

DATA AVAILABILITY

- The data that support the findings of this study are available from the corresponding author, Mohamed Faradji, upon reasonable request.

REFERENCES

[1] A. T. Dahiru, D. Daud, C. W. Tan, Z. T. Jagun, S. Samsudin, and A. M. Dobi, "A comprehensive review of demand side management in distributed grids based on real estate perspectives," *Environmental Science and Pollution Research*, vol. 30, no. 34, pp. 81984–82013, Jan. 2023, doi: 10.1007/s11356-023-25146-x.

[2] M. S. Bakare, A. Abdulkarim, M. Zeeshan, and A. N. Shuaibu, "A comprehensive overview on demand side energy management towards smart grids: challenges, solutions, and future direction," *Energy Informatics*, vol. 6, no. 1, Mar. 2023, doi: 10.1186/s42162-023-00262-7.

[3] T. M. Layadi, G. Champenois, and M. Mostefai, "Economic and ecological optimization of multi-source systems under the variability in the cost of fuel," *Energy Conversion and Management*, vol. 177, pp. 161–175, Dec. 2018, doi: 10.1016/j.enconman.2018.09.056.

[4] R. İ. Kayaalp, M. U. Cuma, and M. Tümay, "A new rule-based self-reconfigurable energy management control of grid and batteries connected hybrid regenerative solar power system for critical loads," *Simulation Modelling Practice and Theory*, vol. 125, p. 102749, May 2023, doi: 10.1016/j.simpat.2023.102749.

[5] S. . Phiri and K. Kusakana, "Demand side management of a grid connected PV-WT-battery hybrid system," in *2016 International Conference on the Industrial and Commercial Use of Energy (ICUE)*, 2016, pp. 45–51.

[6] S. S. Reka and V. Ramesh, "Demand side management scheme in smart grid with cloud computing approach using stochastic dynamic programming," *Perspectives in Science*, vol. 8, pp. 169–171, Sep. 2016, doi: 10.1016/j.pisc.2016.04.024.

[7] M. H. Amrollahi and S. M. T. Bathaee, "Techno-economic optimization of hybrid photovoltaic/wind generation together with energy storage system in a stand-alone micro-grid subjected to demand response," *Applied Energy*, vol. 202, pp. 66–77, Sep. 2017, doi: 10.1016/j.apenergy.2017.05.116.

[8] N. Javaid *et al.*, "A hybrid genetic wind driven heuristic optimization algorithm for demand side management in smart grid," *Energies*, vol. 10, no. 3, p. 319, Mar. 2017, doi: 10.3390/en10030319.

[9] A. U. Rehman *et al.*, "Efficient energy management system using firefly and harmony search algorithm," in *Advances on Broad-Band Wireless Computing, Communication and Applications*, vol. 12, Springer International Publishing, 2018, pp. 37–49.

[10] R. K. Yadav, V. S. Bhadoria, and P. N. Hrisheekesha, "Demand side management using ant colony optimization algorithm in renewable energy integrated smart grid," *Journal of Intelligent and Fuzzy Systems*, vol. 46, no. 4, pp. 7627–7642, Apr. 2024, doi: 10.3233/JIFS-234281.

[11] S. Rahim *et al.*, "Ant colony optimization based energy management controller for smart grid," in *Proceedings - International Conference on Advanced Information Networking and Applications, AINA*, Mar. 2016, vol. 2016-May, pp. 1154–1159, doi: 10.1109/AINA.2016.163.

[12] A. S. O. Ogunjuyigbe, T. R. Ayodele, and O. A. Akinola, "User satisfaction-induced demand side load management in residential buildings with user budget constraint," *Applied Energy*, vol. 187, pp. 352–366, Feb. 2017, doi: 10.1016/j.apenergy.2016.11.071.

[13] N. Javaid *et al.*, "An intelligent load management system with renewable energy integration for smart homes," *IEEE Access*, vol. 5, pp. 13587–13600, 2017, doi: 10.1109/ACCESS.2017.2715522.

[14] N. Kinhekar, N. P. Padhy, F. Li, and H. O. Gupta, "Utility oriented demand side management using smart AC and micro DC grid cooperative," *IEEE Transactions on Power Systems*, vol. 31, no. 2, pp. 1151–1160, Mar. 2016, doi: 10.1109/TPWRS.2015.2409894.

[15] I. Ullah and S. Hussain, "Time-constrained nature-inspired optimization algorithms for an efficient energy management system in smart homes and buildings," *Applied Sciences*, vol. 9, no. 4, p. 792, Feb. 2019, doi: 10.3390/app9040792.

[16] G. R. Hemanth, S. C. Raja, J. J. D. Nesamalar, and J. S. Kumar, "Cost effective energy consumption in a residential building by implementing demand side management in the presence of different classes of power loads," *Advances in Building Energy Research*, vol. 16, no. 2, pp. 145–170, Apr. 2022, doi: 10.1080/17512549.2020.1752799.

[17] V. Jayadev and K. S. Swarup, "Optimization of microgrid with demand side management using genetic algorithm," in *IET conference on power in unity: A whole system approach*, 2013, vol. 2013, no. 15377, pp. 1–12, doi: 10.1049/ic.2013.0124.

[18] S. Li *et al.*, "A deep reinforcement learning-based approach for the residential appliances scheduling," *Energy Reports*, vol. 8, pp. 1034–1042, Aug. 2022, doi: 10.1016/j.egyr.2022.02.181.

[19] A. F. Meyabadi and M. H. Deihimi, "A review of demand-side management: reconsidering theoretical framework," *Renewable and Sustainable Energy Reviews*, vol. 80, pp. 367–379, Dec. 2017, doi: 10.1016/j.rser.2017.05.207.

[20] M. Zeeshan and M. Jamil, "Adaptive moth flame optimization based load shifting technique for demand side management in smart grid," *IETE Journal of Research*, vol. 68, no. 1, pp. 778–789, Feb. 2022, doi: 10.1080/03772063.2021.1886607.

[21] K. Parvez *et al.*, "Scheduling of appliances in HEMS using elephant herding optimization and harmony search algorithm," in *Advances on Broad-Band Wireless Computing, Communication and Applications*, vol. 12, 2018, pp. 62–72.

[22] Niharika and V. Mukherjee, "Day-ahead demand side management using symbiotic organisms search algorithm," *IET Generation, Transmission and Distribution*, vol. 12, no. 14, pp. 3487–3494, Jun. 2018, doi: 10.1049/iet-gtd.2018.0106.

[23] A. C. Batista and L. S. Batista, "Demand side management using a multi-criteria ϵ-constraint based exact approach," *Expert Systems with Applications*, vol. 99, pp. 180–192, Jun. 2018, doi: 10.1016/j.eswa.2018.01.040.

[24] I. Ullah, I. Hussain, and M. Singh, "Exploiting grasshopper and Cuckoo search bio-inspired optimization algorithms for industrial energy management system: Smart industries," *Electronics (Switzerland)*, vol. 9, no. 1, p. 105, Jan. 2020, doi: 10.3390/electronics9010105.

[25] R. K. Yadav, P. N. Hrishikesha, and V. S. Bhadoria, "Lowest tariff load shifting demand side management technique in smart grid environment," *International Journal of Social Ecology and Sustainable Development*, vol. 13, no. 2, pp. 1–16, Jun. 2022, doi: 10.4018/IJSESD.302468.

[26] T. M. Layadi, G. Champenois, M. Mostefai, and D. Abbes, "Lifetime estimation tool of lead-acid batteries for hybrid power sources design," *Simulation Modelling Practice and Theory*, vol. 54, pp. 36–48, May 2015, doi: 10.1016/j.simpat.2015.03.001.

[27] T. M. Layadi, G. Champenois, M. Mostefai, I. Colak, and K. Kayisli, "Design of sustainable multi-source power systems using lithium batteries," *Journal of Energy Storage*, vol. 60, p. 106648, Apr. 2023, doi: 10.1016/j.est.2023.106648.

[28] Y. Song, Y. Liu, H. Chen, and W. Deng, "A multi-strategy adaptive particle swarm optimization algorithm for solving optimization problem," *Electronics (Switzerland)*, vol. 12, no. 3, p. 491, Jan. 2023, doi: 10.3390/electronics12030491.

[29] D. Karaboga and E. Kaya, "Adaptive network based fuzzy inference system (ANFIS) training approaches: a comprehensive survey," *Artificial Intelligence Review*, vol. 52, no. 4, pp. 2263–2293, Jan. 2019, doi: 10.1007/s10462-017-9610-2.

[30] T. Logenthiran, D. Srinivasan, and T. Z. Shun, "Demand side management in smart grid using heuristic optimization," *IEEE Transactions on Smart Grid*, vol. 3, no. 3, pp. 1244–1252, Sep. 2012, doi: 10.1109/TSG.2012.2195686.

BIOGRAPHIES OF AUTHORS

Mohamed Faradji 🆔 �— SC ◑ received his masters degree in telecommunication systems from Yahia Fares University of Medea, in 2019. He is Ph.D. student at M'Hamed Bougara University in Boumerdes since 2019. He was a visiting researcher at Nisantasi University in Turkey. His current interests include smart grid simulation and optimization, load frequency and voltage control, and artificial neural network implementation. He can be contacted at email: m.faradji@univ-boumderes.dz.

Toufik Madani Layadi 🆔 �— SC ◑ was born in Bordj Bou Arreridj, Algeria. He received his engineering diploma in automatic control from the department of electrical engineering, University of Setif, Algeria in 2004. He obtained his magister degree in electronics control from the department of electronics, University of Setif in 2007. He received his Ph.D. degree in automatic control from the electrical engineering department, Setif University-Algeria, and Poitier University-France in 2016. He received his HDR diploma from the department of electrical engineering, University of Setif in 2019. Currently, he is working as an associate professor since 2009 in the department of electromechanical at Mohammed Elbachir El-Ibrahimi University, Bordj Bou Arréridj-Algeria. His research interests concern design and optimization of multi-source systems, and lead-acid and lithium battery technologies. Also, he interested in renewable energy sources and electric vehicles. He can be contacted at email: toufikmadani.layadi@univ-bba.dz

Khaled Rouabah 🆔 �— SC ◑ received his engineering degree in electronics from the University of Farhat Abbas, Setif, Algeria, in 1999. He obtained his master's degree in telecommunications and networking in 2001 from Higher Institute of Aeronautics and Space, Toulouse, France, his magister degree in communications and his Ph.D. degree in electronics engineering from the University of Farhat Abbas, Setif, Algeria, in 2005 and 2010 respectively. In 2013, he obtained his HDR degree in electronics in Mohamed Boudiaf University of Msila. Between July 2018 and October 2022, he worked as a professor in the Department of Electronics at Mohamed EL Bachir El Ibrahimi University, Bordj Bou Arreridj. He is currently holding the same position at the Electronics Department of Mohamed Boudiaf University of Msila. His research interests include communication signals, geolocation, parallel processing, pattern recognition, hardware implementation, signal structure design, mobile computing, and telecommunications networks. He can be contacted at email: rouabahkha@gmail.com.